J. Ocean Univ. China (Oceanic and Coastal Sea Research)
https://doi.org/10.1007/s11802-025-5985-x
ISSN 1672-5182, 2025 24 (3): 707-720
http://www.ouc.edu.cn/xbywb/
E-mail:xbywb@ouc.edu.cn

Differences of Morphology and Muscle Transcriptomes Reveal the Individual Difference of Swimming Performance in Juvenile Spotted Sea Bass (*Lateolabrax maculatus*)

LI Haoyang[#], LI Hao[#], LI Chengtian, JIN Xi, LI Weiwei, WEN Haishen, LI Yun, LAI Qianyan, NIU Chunxiang, and QI Xin[*]

Key Laboratory of Mariculture, *Ministry of Education* (*KLMME*), *Fisheries College*, *Ocean University of China*, *Qingdao* 266003, *China*

(Received April 30, 2024; revised July 13, 2024; accepted October 11, 2024)

Abstract Deep-sea aquaculture is an emerging trend due to the contamination and overexploitation of nearshore mariculture areas. However, the complex water conditions in the deep sea impose higher demands on the swimming performance of farmed animals. Spotted sea bass (*Lateolabrax maculatus*) is one of the most economically important fish species in China. To investigate the mechanisms underlying the individual variations in swimming performance among spotted sea bass, we measured their critical swimming speed (U_{crit}) and morphological phenotypes. Total length, body length, body weight, caudal region length, and condition factor showed significant positive correlations with absolute U_{crit}. In contrast, caudal fin length and pectoral fin length tended to hinder the swimming performance of individual spotted sea bass. Additionally, white muscle tissues from fish exhibiting good swimming performance (relative U_{crit}>8.20 BL/s) and poor swimming performance (relative U_{crit}<7.31 BL/s) were sampled for RNA-seq. A total of 694 differential expression genes (DEGs) were identified through gene expression analysis, with significant enrichment in GO terms such as mitochondrial protein complex, ribosomal subunit, structural constituent of ribosome, and oxidative phosphorylation, as well as genes in KEGG pathways including ribosome and metabolic pathways. In conclusion, our study for the first time comprehensively elucidated the impact of morphology of spotted sea bass on its individual differences in swimming ability, and analyzed the genetic basis underlying swimming ability using transcriptomic methods. This study provides a theoretical basis for the potential breeding varieties of spotted sea bass suitable for deep-sea aquaculture.

Key words spotted sea bass; critical swimming speed; morphology; RNA-seq

1 Introduction

Fish is a crucial component of the aquatic products industry in China. In 2022, the national aquaculture production of China reached 55.65 million tons, with fish production accounting for over the half at 29.03 million tons (Ministry of Agriculture and Rural Affairs, 2023). Fish is rich in high-quality protein and essential nutrients such as PUFA, vitamins, and minerals (Xie *et al*., 2022). Unlike freshwater fishes, marine fishes are nearly odorless (Tetsuo Kawai, 1996). Due to these advantages, there is a continuous increase in the demand for marine fishes (Long *et al*., 2024). Nonetheless, the rapid expansion of nearshore aquaculture has led to significant space occupation and environmental challenges in marine fish farming, necessitating the establishment of deeper offshore farms employing advanced technology and cultivation methods (Gentry *et al*., 2017; Zhu *et al*., 2023). Nevertheless, complex underwater environments pose numerous obstacles for deep-sea aquaculture, including strong waves and swift currents (Dong *et al*., 2008; Zhang and Liu, 2018; Chen *et al*., 2019). High water velocities can induce fatigue in farmed fish and negatively impact their growth, creating a need to select fish species with improved swimming capabilities to thrive in these dynamic conditions (Yuan *et al*., 2023). Moreover, due to constraints such as body size, growth rate, bait availability, and market demand, the careful selection of appropriate species for deep-sea aquaculture holds significant importance (Zhang and Liu, 2018).

Swimming performance is an essential behavior that facilitates fish in capturing prey and evading predators, playing a crucial role in their survival, growth, and reproduction (Li *et al*., 2023). Additionally, swimming performance has a significant impact on fish welfare and muscle quality (Timmerhaus *et al*., 2021). Compared to those with poor swimming performance, fishes with good swimming performance were reported to exhibit greater disease resistance, and faster recovery from acute stress (McKen-

[#] The two authors contributed equally to this work.

* Corresponding author. E-mail: qx@ouc.edu.cn

zie *et al*., 2012; Castro *et al*., 2013). It's obvious that swimming is a critical determinant of fish fitness (Martinez *et al*., 2003). Fish swimming can be classified into three major categories based on swimming speed and time, including sustained swimming, prolong swimming, and burst swimming (Hammer, 1995; Martinez *et al*., 2003; Gui *et al*., 2014). Among these categories, sustained swimming capacity is essential for fish to thrive in offshore environments (Hvas *et al*., 2021). Critical swimming speed (U_{crit}), primarily focusing on aerobic endurance, can be used as an indicator to represent the estimated sustained swimming capacity with regards to strong current events at exposed aquaculture sites (Reidy *et al*., 2000; Hvas *et al*., 2021).

Swimming performance of fish is reported to be influenced by their morphological phenotypes , oxygen supply, and energy metabolism (McClelland *et al*., 2006; Ohlberger *et al*., 2006; Domenici *et al*., 2013; Rubio-Gracia *et al*., 2020; Chen *et al*., 2022). However, the impact of morphological phenotypes on swimming performance varies among fish species. For instance, in Atlantic cod (*Gadus morhua*), absolute U_{crit} showed no correlation with fin surface, fork length and mass (Reidy *et al*., 2000). In contrast, another study conducted on largemouth bass (*Micropterus salmoides*) showed that morphological measurements accounted for 79.8% of the individual variance in swimming ability (Jhonnerie *et al*., 2023). Moreover, a few studies were conducted to investigate the genetic basis of fish swimming. Swimming performance was found to be heritable in Nile tilapia (*Oreochromis niloticus*), and large yellow croaker (*Larimichthys crocea*) (Mengistu *et al*., 2021; Zeng *et al*., 2022). Genetic differences linked to swimming physiology, regulation of swimming behavior, and oxygen intake were identified in the white muscle transcriptomes of different cichlid fishes (Raffini *et al*., 2020). There is still a significant knowledge gap in explaining the genetic basis of fish swimming performance. Therefore, conducting morphology-based and genetics-based research on individual differences in fish swimming performance is worthwhile.

Spotted sea bass (*Lateolabrax maculatus*) is a eurysaline and eurythermic fish species found in East Asia (Zhang *et al*., 2017; Liu *et al*., 2020). These characteristics enable spotted sea bass to inhabit with a wide ecological range, including the coastlines and estuaries of China, Japan, and the Korean Peninsula (Liu *et al*., 2006; Liu *et al*., 2020; Sun *et al*., 2024). The remarkable ability of spotted sea bass to adapt to diverse and complex conditions present potential for its deep-sea aquaculture. Moreover, spotted sea bass holds significant economic importance as a fishery species in China (Li *et al*., 2019). In 2022, the annual production of maricultured spotted sea bass in China reached 218053 tons, accounting for 11.32% of the total output of maricultured fish in the country, indicating its robust market demands (Ministry of Agriculture and Rural Affairs, 2023).

This study aimed to investigate the mechanisms underlying the variations in swimming performance among spotted sea bass individuals from both morphological and molecular perspectives. In fish, swimming is a complex activity requiring the involvement of multiple organs, such as the brain, gills, heart, muscles and so on. However, as the locomotive organ, muscles play a critical role in converting chemical energy into kinetic energy (Barclay, 2019). Moreover, studies on athletics performances are mainly focused on muscles, including how muscular strength impacts athletic performance, changes in muscle related to age, plasticity of skeletal muscle in response to various exercise modes and so on, which reflects the important role of muscle in exercise physiology (Faulkner *et al*., 2008; Suchomel *et al*., 2016; Furrer *et al*., 2023). Therefore, the muscle was chosen as the research target. In the present study, the swimming performance and morphological phenotypes of individual spotted sea bass juveniles were measured and analyzed. Additionally, white muscle samples were collected from individuals with different swimming performances for RNA-Seq analysis. This study established a foundation for understanding swimming performance in spotted sea bass and provided theoretical support for selecting optimal breeds for deep-sea aquaculture.

2 Materials and Methods

2.1 Experimental Fish

A total of 862 experimental spotted sea bass were acquired from Yantai Jinghai Marine Fishery Co., Ltd. (Yantai, China), with an average body weight of 5.97 g±1.32 g and an average body length of 7.34 cm±0.54 cm. The fish were maintained in a recirculating water system at Ocean University of China (Qingdao, China). During acclimation, the salinity of the water was gradually reduced from 30 to 0 (approximately 10 per day) by adding fresh water, and the fish were kept in fresh water (pH=7.54) for 2 weeks. The water temperature was maintained at approximately 18 °C, and the dissolved oxygen saturation was consistently maintained above 80%. The fish were not fed for 48 h prior to the experiment.

2.2 U_{crit} Test

The critical swimming speed (U_{crit}) of fish was assessed by using the circulating water channel at Ocean University of China (Figs.1a–b) (Brett, 1964; Raffini *et al*., 2020; Yan *et al*., 2022; Li *et al*., 2023). And the fish were placed inside a net cage that measured 1 m in length, 0.5 m in width, and 0.25 m in height (Figs.1a–b). Water velocities at various locations within the net cage were measured using a flow meter (XiangRuiDe LS300-A, China), ensuring a variance within 1 cm. For each trial, a random selection of 50–70 fish were introduced into the net cage within the swimming channel. Prior to the experiment, the fish were acclimated in the net cage for 30 min at a low water velocity of 10 cm/s. Subsequently, the water velocity was incrementally raised by 5 cm/s every 5 min until it reached 25 cm/s (approximately half of the estimated absolute U_{crit}). Then the water velocity was increased by 10 cm/s every 15 min until all the fish became fatigued. Fa-

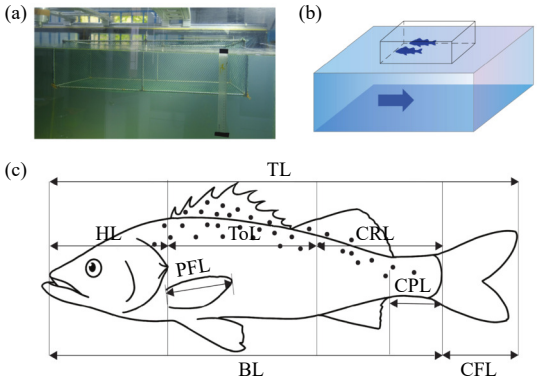

Fig.1 Overview of the net cage, circulating water channel, and the position of the morphological parameters measured in this study. (a) Photograph showing the testing area of the water channel and net cage. (b) Diagram of the net cage and water channel used for critical swimming speed tests. The dark blue arrow represents the direction of water flow. (c) Eight morphological parameters of spotted sea bass were measured in this study. HL, head length; ToL, torso length; CRL, caudal region length; CPL, caudal peduncle length; CFL, caudal fin length; PFL, pectoral fin length; BL, body length; TL, total length.

tigue was determined by the inability of fish to swim forward and their drifting back towards the rear of the cage. The experiment ended when all the tested fish in each batch exhibited signs of fatigue, which occurred approximately 120 min after the formal start of experiment. U_{crit} was calculated using Brett's equation (Brett, 1964): absolute $U_{crit}=U_1+(T_1/T_2)\times U_2$, relative U_{crit}=absolute U_{crit}/BL (body length). Here, U_1 represents the highest water velocity at which the fish could swim throughout the entire time interval, T_1 denotes the duration of fish swimming at the highest water velocity before fatigue, T_2 refers to the time interval between water velocity increments, U_2 is the water velocity increment.

2.3 Morphological Phenotypes Acquisition

To investigate the impact of different morphological phenotypes of spotted sea bass on their swimming performance, tpsdig2 v2.32 was utilized to measure morphological parameters based on individual images. The morphological parameters analyzed in this study comprised body weight (BW), total length (TL), body length (BL), head length (HL), torso length (ToL), caudal region length (CRL), caudal peduncle length (CPL), caudal fin length (CFL), and pectoral fin length (PFL) (Fig.1c).

2.4 Group Setting and Sample Collection

In order to investigate the genetic basis of swimming performance in spotted sea bass, an additional U_{crit} test was conducted on 42 fish using the same protocol as described in section 2.2 with a few modifications. After the water velocity reached 25 cm/s, the duration of each velocity increment was set to 30 min in order to amplify the variation in swimming performance among individuals.

Individuals with relative U_{crit} over 8.20 BL/s were grouped into the good swimmers (G) group (n=6), while fish with relative U_{crit} under 7.31 BL/s were grouped into the poor swimmers (P) group (n=6). The fish were anesthetized with MS-222 (200 mg/L), and thereafter the white muscles from the same region of fish back were collected and were immediately transferred to liquid nitrogen for rapid freezing. The samples were then stored at −80 °C for RNA extraction.

2.5 RNA Extraction and Transcriptome Sequencing

The white skeletal muscle samples (n=3 for each group) were homogenized and the total RNA was extracted using Trizol reagent (Invitrogen, USA) following the manufacturer's instructions. The RNA concentration was determined using the Biodropsis BD-1000 nucleic acid analyzer (OSTC, China), while the integrity of the RNA was assessed using the Agilent 2100 Bioanalyzer system (Agilent Technologies, USA).

mRNA was purified from total RNA using poly-T oligo-attached magnetic beads and fragmented under elevated temperature. cDNA fragments were synthesized using a random hexamer primer, M-MuLV Reverse Transcriptase (RNase H), DNA Polymerase I, and RNase H. Following amplification and purification, the highly qualified libraries were pooled and subjected to sequencing on Illumina platforms using the PE150 strategy by Novogene Co., Ltd. (Beijing, China).

2.6 Identification of Differential Expression Genes (DEGs)

Through the use of Fastp v0.23.1, the qualities of raw reads were evaluated and high quality clean reads were obtained by removing pair reads with adapter contamination and low-quality sequences. The clean reads were aligned to the *L. maculatus* reference genome (JAYMH B000000000) using hisat2 v2.2.1 (Kim *et al*., 2015; Chen *et al*., 2018). The software samtools v1.17 was employed to convert the alignment format of the mapped data from SAM to BAM (Li *et al*., 2009). Thereafter, featureCounts of subread v2.0.6 was utilized to quantify the number of exons covered by the clean reads mapped to functional genes (Liao *et al*., 2014).

Counts were subjected to DESeq2 R package v1.40.2 for raw counts normalization and differential expression genes (DEGs) identification (Anders and Huber, 2010). A threshold of P-adjust<0.05 and $|\log_2 FC|>1$ (FC, fold change) was utilized to determine the DEGs of spotted sea bass with different swimming performance (Love *et al*., 2014). Additionally, the ggplot2 v3.4.3 R package was utilized to generate volcano plots and heatmaps.

2.7 GO and KEGG Enrichment Analyses of DEGs

Gene ontology (GO) enrichment analysis of the DEGs was performed by using the OmicShare online software (https://www.omicshare.com/tools/Home/Soft/gogseasenior). Kyoto Encyclopedia of Genes and Genomes (KEGG) pathway analysis of the DEGs was implemented by using

KOBAS (http://bioinfo.org/kobas) (Bu *et al*., 2021). The analyses results were visualized using R Studio v3.4.3.

2.8 RT-qPCR Validation of RNA-Seq Data

To validate the veracity of the RNA-Seq analysis results, RT-qPCR was performed to measure the expression levels of 9 differential expression genes (*gatc*, *ndufb3*, *rasl11b*, *ndufa13*, *asb16*, *tmsb2*, *dyrk2*, *si:ch211-171h4.3*, and *dnajb5*). And *18S ribosomal RNA* (*18S*) gene was used as the endogenous reference gene for RT-qPCR normalization (Wang *et al*., 2018). The cDNA templates were synthesized from the RNA of each sample using the *Evo M-MLV* RT Mix Kit with gDNA Clean for qPCR Ver.2 (Accurate Biotech, China) according to the manufacturer's protocol. The specific primers used for RT-qPCR were designed using Primer-BLAST and were verified with TBtools-II v2.065 (Chen *et al*., 2023). The detailed information of primer sequences is provided in Table 1.

RT-qPCR was performed using the StepOne Plus Real-Time PCR system (Applied Biosystems), and each sample was run in triplicate. Each 10 μL reaction system consisted of 2 μL cDNA template, 0.2 μL of each forward/reverse primer, 5 μL of 2× ChamQ SYBR qPCR Master Mix (High ROX Premixed) (Vazyme, China), and 2.6 μL of ddH_2O. The qPCR amplification program consisted of an initial denaturation step at 95 °C for 30 s, followed by 40 cycles at 95 °C for 10 s, and 60 °C for 30 s.

2.9 Statistical Analyses

For morphological phenotypes acquisition, additional parameters such as condition factor (CF, calculated as the ratio of BW to BL), CPL+CFL, HL/TL, ToL/TL, CRL/TL, CPL/TL, CFL/TL, PFL/TL and (CPL+CFL)/TL were computed and analyzed to explore the relationship between more complex morphological parameters and absolute U_{crit}. Data analysis and visualization were performed using R packages, specifically ggplot2 v3.4.3, ggridges v0.5.6, and corrplot v0.92.

The $2^{-\Delta\Delta CT}$ method was used to compute the relative expression levels in RT-qPCR (Livak and Schmittgen, 2001). The correlation coefficient between the $\log_2$FC in RNA-Seq group and the RT-qPCR group was determined using SPSS v25.0.

3 Results

3.1 Swimming Performance of the Juveniles of Spotted Sea Bass

To better understand the relationship between swimming performance and morphology, a total of 820 fish were used for swimming test and pictured to acquire morphological phenotypes. The absolute U_{crit} values for all spotted sea bass juveniles were determined to be between 24.50 cm/s and 61.72 cm/s, with an average absolute U_{crit} of (42.03±7.32) cm/s (mean±SD.) (Fig.2a).

3.2 Morphology Phenotypes Correlated with U_{crit}

Eighteen morphological descriptors were measured on the left side of 765 fish, with 55 fish discarded due to quality control issues and missing data. The distributions of all these parameters were depicted in Figs.2b–d, indicating approximately normal distributions for these parameters. A summary of the morphological phenotype was presented in Table 2.

To enhance our understanding of the relationship between morphological phenotypes and swimming performance, a correlation analysis was conducted (Fig.3). Generally, absolute U_{crit} exhibited a positive correlation with TL, BL, BW, HL, ToL, CRL, CPL, CFL, CPL+CFL and

Table 1 Summary of the genes used for RT-qPCR validation with their primers

Gene name	Accession number of NCBI	Classification	Primer (5'→3')	Tm (°C)	Product size (bp)
18S ribosomal RNA	JN211898	Reference gene	F: GGGTCCGAAGCGTTTACT R: TCACCTCTAGCGGCACAA	57.00 58.21	179
gatc	PQ487270	Down	F: GGACTGTGCCGAAGAACTGC R: CCTCTCCTCCCGCTTTGGTAG	61.57 61.91	100
ndufb3	PQ487271	Down	F: ATGGCCACAGCAAGATGTCC R: AACCTCCAAGCCTCGTTTCG	60.68 60.60	133
rasl11b	PQ487272	Down	F: AGGCGCTTCATCGGAGACTA R: ATCAGTCATCTCCACGCCAG	60.75 59.54	120
ndufa13	PQ487273	Down	F: TTGTGGAGAAGGCAGGAGGAAG R: TGTGTAGTGTAAGTACCCGAGAGTC	61.95 61.31	132
asb16	PQ487274	Down	F: TACACGCCGATGGACTGTCT R: ATCGCGCTATTTCTTCCGGT	60.96 59.90	73
tmsb2	PQ487275	Up	F: GCAGATTCACTCAGCTTCCTCATC R: GTTCCACCAGCGGCGAGAG	61.51 63.28	82
dyrk2	PQ487276	Up	F: GCGCCAGAGGTCATTCTAGG R: AGGCGTCTAGGAGCTTCTGC	60.25 61.67	178
si:ch211-171h4.3	PQ487277	Up	F: AGGTCTGGTACAGCTCTCCTT R: GGAAACCCAAACTCTTCGTCT	59.92 58.15	131
dnajb5	PQ487278	Up	F: AGAGGAAGGTTTGAAGACGGGAG R: ACGTGTAGTGGTATGTCGAGC	61.88 59.87	71

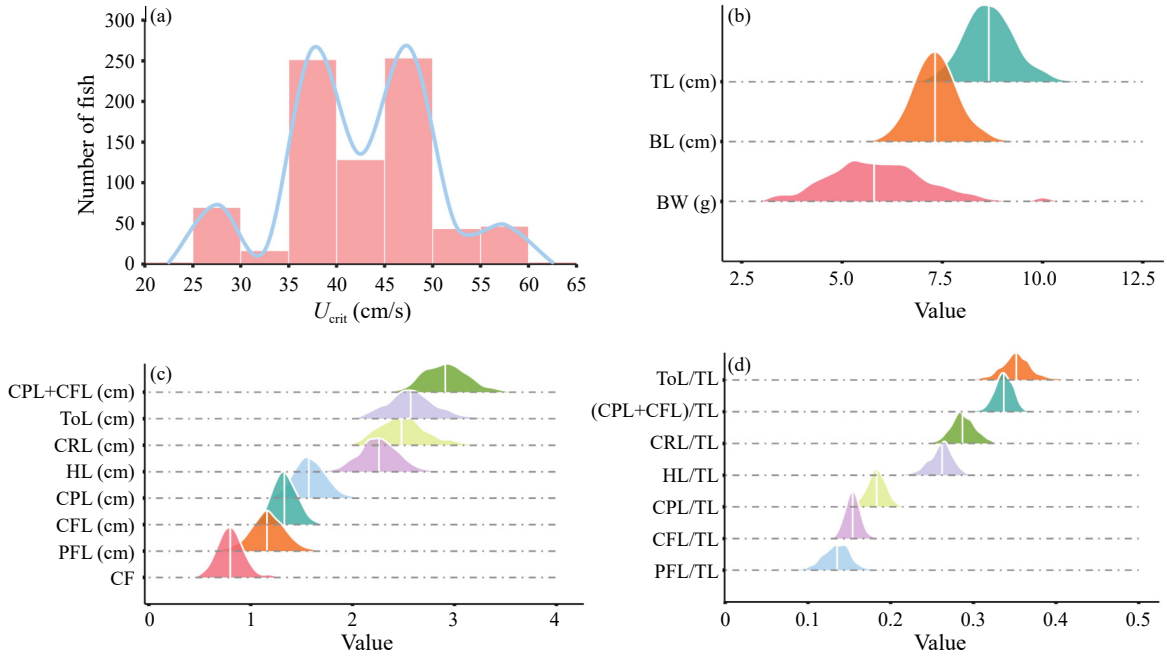

Fig.2 Distribution of swimming performance and morphological parameters of spotted sea bass juveniles. (a) The distribution of absolute U_{crit} of juvenile spotted sea bass. (b) The distribution of total length (TL), body length (BL), and body weight (BW). (c) The distribution of caudal peduncle length+caudal fin length (CPL+CFL), torso length (ToL), caudal region length (CRL), head length (HL), caudal peduncle length (CPL), caudal fin length (CFL), pectoral fin length (PFL), and condition factor (CF). (d) The distribution of ToL/TL, (CPL+CFL)/TL, CRL/TL, HL/TL, CPL/TL, CFL/TL, and PFL/TL. The *x*-axis shows the value of each parameter, while the *y*-axis shows the number of juveniles.

Table 2 Summary of the morphological parameters of 765 spotted sea bass juveniles

Parameter	Max	Min	Mean±SD
TL (cm)	10.83	6.98	8.68±0.63
BL (cm)	9.26	5.91	7.34±0.54
HL (cm)	2.94	1.74	2.26±0.19
HL/TL	0.32	0.20	0.26±0.02
ToL (cm)	3.77	1.85	2.59±0.25
ToL/TL	0.48	0.28	0.35±0.02
CRL (cm)	3.29	1.33	2.49±0.24
CRL/TL	0.35	0.16	0.29±0.02
CPL (cm)	2.62	1.17	1.59±0.16
CPL/TL	0.30	0.12	0.18±0.01
CFL (cm)	1.95	1.00	1.34±0.12
CFL/TL	0.21	0.12	0.15±0.01
PFL (cm)	1.71	0.56	1.17±0.17
PFL/TL	0.19	0.06	0.14±0.02
CPL+CFL (cm)	3.94	2.35	2.92±0.22
(CPL+CFL)/TL	0.29	0.45	0.34±0.01
BW (g)	11.50	3.20	5.96±1.33
CF	1.28	0.49	0.81±0.13

CF. Among these impacts, BL and TL demonstrated the highest correlation with absolute U_{crit} (correlation coefficient, BL: 0.40, TL: 0.40, *P*-value<0.05). In addition, a subtle positive correlation was observed between PFL and absolute U_{crit} though this trend was not statistically significant (Fig.3). Moreover, to better understand the effects of the length of each body part on swimming performance, the variations of individual total length were taken into consideration. CRL/TL showed a positive correlation with absolute U_{crit}, though the correlation coefficient was lower than that between CRL and absolute U_{crit} (CRL/TL: 0.12, CRL: 0.37). Moreover, the CFL/TL, PFL/TL and (CPL+CFL)/TL showed significant negative correlations with absolute U_{crit} (CFL/TL: −0.13, (CPL+CFL)/TL: −0.10, *P*-value<0.05), which was completely opposite to the relation between their counterparts and absolute U_{crit}, indicating that relatively longer individual CFL and PFL may reverse its positive role in swimming performance.

3.3 Quality of Library Construction and Assembly

Fish with relative U_{crit} ranking at the top and the bottom of the test population were selected and categorized as good swimmers group (G) (relative U_{crit}≥8.20 BL/s) and poor swimmers group (P) (relative U_{crit}≤7.31 BL/s). The body weight (*t*-test, *P*-value=1), body length (*P*-value=0.65), and total length (*P*-value=0.64) among these two groups showed no significant differences. The white muscles of spotted sea bass juveniles in the good and poor swimmers groups were sampled and three transcriptome of each group were obtained using Illumina RNA-Seq (Table 3). The number of raw reads in each library ranged from 40.60 million to 47.03 million. There were a total of 129.79 million raw reads in the good swimmers group, while 125.66 million raw reads in the poor swimmers group. The percentage of Q20 and Q30 bases in all samples exceeded 97.03 and 92.92, respectively. After filtering pair reads with adapter contamination and low-quality sequences, libraries produced 39.22 million to 45.54 million clean reads. There were 127.12 million clean reads in the good swimmers group, and the poor swimmers group

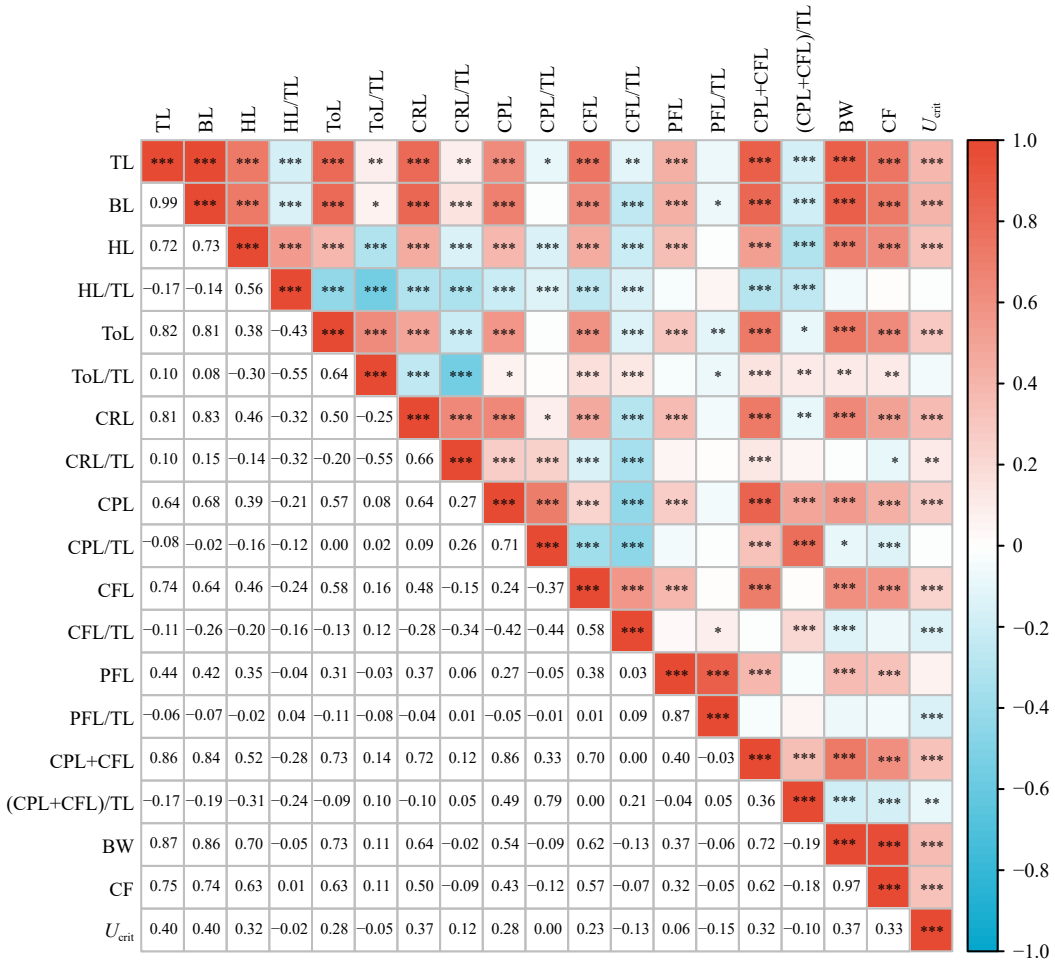

Fig.3 Heatmap of the relationship between morphological parameters and absolute U_{crit}. Correlation coefficients lower than 0 are presented in blue color, while correlation coefficients higher than 0 are presented in red color; the number in data frame represents correlation coefficient; *** indicates *P*-value<0.001, ** indicates *P*-value<0.01, * indicates *P*-value<0.05.

Table 3 Summary of the transcriptome sequencing data

Samples	G1	G2	G3	P1	P2	P3
Raw reads	47025756	42162924	40602510	43465250	42073266	41580574
Clean reads	45536374	40907756	39215998	42527384	41160906	40509914
Raw base (G)	7.05	6.32	6.09	6.52	6.31	6.24
Clean base (G)	6.83	6.14	5.88	6.38	6.17	6.08
Effective (%)	96.83	97.02	96.59	97.84	97.83	97.43
Error (%)	0.03	0.03	0.03	0.02	0.03	0.02
Q20 (%)	97.03	97.55	97.69	97.93	97.9	98
Q30 (%)	92.92	93.46	93.88	94.27	94.16	94.41
GC (%)	51.9	50.89	51.62	50.24	50.11	50.37
Total mapped	42235024	36521800	36074801	40477968	39445927	38322205
Mapped rate (%)	92.75	89.28	91.99	95.18	95.83	94.60

had 124.20 million clean reads.

After aligned with reference genome, the total number of mapped reads of each sample ranged from 38.32 million to 42.24 million, and the mapping rate for each transcriptome was between 89.28% and 95.83%. The good swimmers group had a total of 114.83 million mapped reads, while the poor swimmers group had 118.25 million mapped reads. Following mapping, a total of 25608 unigenes were identified in each library. The sequences of the raw reads from RNA-Seq were submitted to the NCBI Sequence Read Archive (SRA) under accession number PRJNA1103656.

3.4 Differential Expression Genes (DEGs) Between Good and Poor Swimmers Group

To identify the DEGs related to swimming ability, transcriptome data from white skeletal muscle of good and poor swimmers were subjected to DESeq analysis. On the basis of adjusted *P*-value<0.05 and $|\log_2 FC|>1$ criteria, a total of 694 DEGs were identified, of which 224 were up-regulated genes (genes had significantly higher expression in poor swimmers group) and 470 were down-regulated

genes (Table 4). Volcano plot depicts the distribution of these DEGs and their variance (Fig.4a). The heatmap clustered the samples into 2 distinct groups (Fig.4b), indicating that the differences in gene expression in the white skeletal muscle were correlated with the variation in swimming performance.

3.5 GO Enrichment Analysis of DEGs

GO enrichment analysis was conducted on 694 DEGs from three classes: biological process (BP), cellular component (CC) and molecular function (MF) (Fig.5). GO enrichment analysis revealed enrichment of DEGs in 7836 terms, out of which 869 terms with a *P*-value<0.05 were considered statistically significant. In these significantly enriched terms, 575 terms belonged to BP class, 126 terms belonged to CC class, and 168 terms belonged to MF class. Among the top 30 significantly enriched GO terms, 13 terms were from BP class: oxidative phosphorylation (GO:0006119, 52 DEGs), mitochondrial ATP synthesis coupled electron transport (GO:0042775, 42 DEGs), ATP synthesis coupled electron transport (GO:0042773, 42 DEGs), ATP metabolic process (GO:0046034, 67 DEGs), electron transport chain (GO:0022900, 51 DEGs) and other terms related to energy metabolism represented in Fig.5. For 16 terms of CC in the top 30 terms, the majority of them were about mitochondria like mitochondrial protein complex (GO:0098798, 83 DEGs) and mitochondrial inner membrane (GO:0005743, 98 DEGs), and related to ribosome component like ribosomal subunit (GO:0044391, 67 DEGs) and ribosome (GO:0005840, 68 DEGs). However, there was only 1 term of class MF enriched in the top 30 terms, namely, the structural constituent of ribosome (GO:0003735, 63 DEGs).

3.6 KEGG Pathway Analysis of DEGs

KEGG analysis was employed to identify the signaling pathways associated with the DEGs. In total 113 pathways were identified, of which 29 were significantly enriched (*P*-value<0.05) (Table 5). According to the KEGG pathway database, the majority of enriched pathways were classified into classes of metabolism and genetic information processing, as depicted in Fig.6. Among the 20 pathways in class Metabolism, 5 pathways were related to amino acid metabolism (cysteine and methionine metabolism, valine, leucine and isoleucine degradation, arginine and proline metabolism, tyrosine metabolism and tryptophan metabolism), and there were also 5 pathways pertain to carbohydrate metabolism (glycolysis/gluconeogenesis, citrate cycle (TCA cycle), pyruvate metabolism, propanoate metabolism and glyoxylate and dicarboxylate metabolism). Furthermore, oxidative phosphorylation and sulfur metabolism pathways are correlated with energy metabolism. Furthermore, cardiac muscle contraction exhibited relatively higher $-\log_{10}$(*P*-value), indicating its potential role in regulating swimming performance. Overall, the results of the KEGG analysis indicated that metabolic processes and gene expression process play important roles in the individual differences of swimming performance.

3.7 RT-qPCR Analysis and Validation

To further validate the accuracy of the Illumina RNA-Seq data, nine genes (*gatc*, *ndufb3*, *rasl11b*, *ndufa13*, *asb16*, *tmsb2*, *dyrk2*, *si:ch211-171h4.3*, and *dnajb5*) were

Table 4 List of top 10 up- and down-regulated DEGs with annotated gene symbol and description

	Gene symbol	Description	$\log_2$FC	*P*-adj
Up-regulated	*si:ch211-171h4.3*	Protein tyrosine kinase	2.689	1.08E-06
	dyrk2	Dual-specificity tyrosine-(Y)-phosphorylation regulated kinase 2	2.325	1.08E-06
	lum	Leucine rich repeat N-terminal domain	2.131	6.39E-06
	LOC125899927	Cell surface proteoglycan that bears heparan sulfate	2.156	1.24E-05
	LOC122888538	Periostin, osteoblast specific factor a	1.743	2.72E-05
	LOC111564635	Peripheral myelin protein	1.574	7.86E-05
	vegfaa	Vascular endothelial growth factor	1.749	1.32E-04
	col6a3	Collagen	1.606	1.34E-04
	LOC104924649	Filamin A interacting protein 1a	2.619	1.42E-04
	LOC127374980	Family with sequence similarity 46, member D	4.628	1.46E-04
Down-regulated	*mrps28*	Ribosomal protein S28	−2.875	1.53E-11
	asb16	Ankyrin repeat and SOCS	−2.771	1.44E-10
	LOC116066953	Alpha-L-fucosidase	−2.257	4.96E-06
	armc2	Armadillo repeat containing 2	−2.493	7.78E-06
	slc3a2a	Solute carrier family 3	−2.226	7.78E-06
	pyurf	PIGY upstream reading frame	−1.969	7.89E-06
	zgc:86896	Functions as component of the Arp2/3 complex which is involved in regulation of actin polymerization and together with an activating nucleation-promoting factor (NPF) mediates the formation of branched actin networks	−4.088	2.58E-05
	LOC122864563	Zinc finger	−2.231	3.03E-05
	cluap1	Clusterin associated protein 1	−1.818	7.86E-05
	LOC118332666	Eukaryotic translation initiation factor	−1.675	9.32E-05

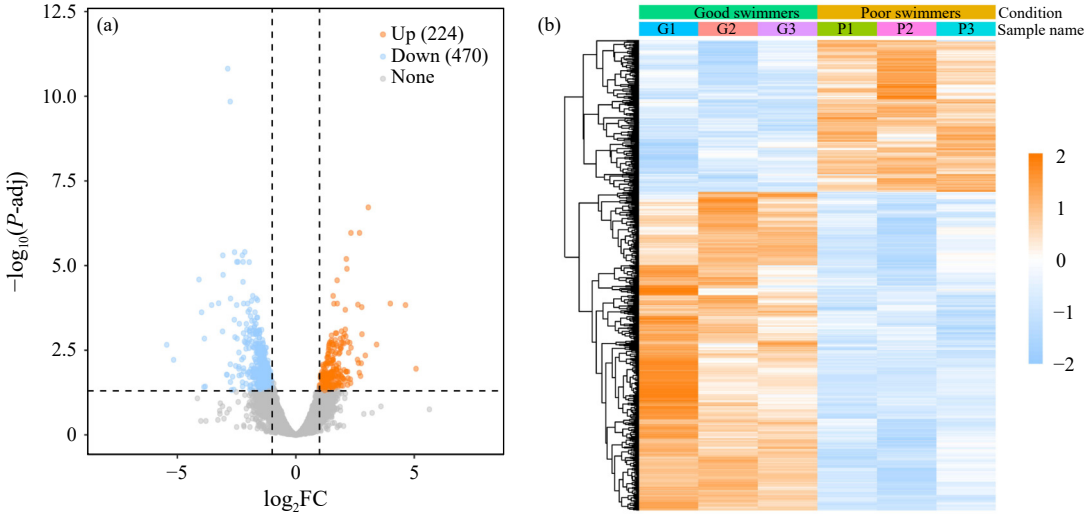

Fig.4 Plots display the differential expression genes (DEGs) of good swimmers and poor swimmers. (a) Volcano plot of DEGs; Blue dots represent down-regulated genes, and orange dots represent up-regulated genes with grey dots represent genes with no significant expression differences between two groups. (b) Heatmap of DEGs function in the skeletal white muscle of spotted sea bass in the good and poor swimmers groups; A total of 694 DEGs are showed in heatmap on the basis of the expression levels of each sample; DEGs expression levels lower than the mean level are showed in blue color while those expression levels exceed mean level are presented in orange color. FC, fold change.

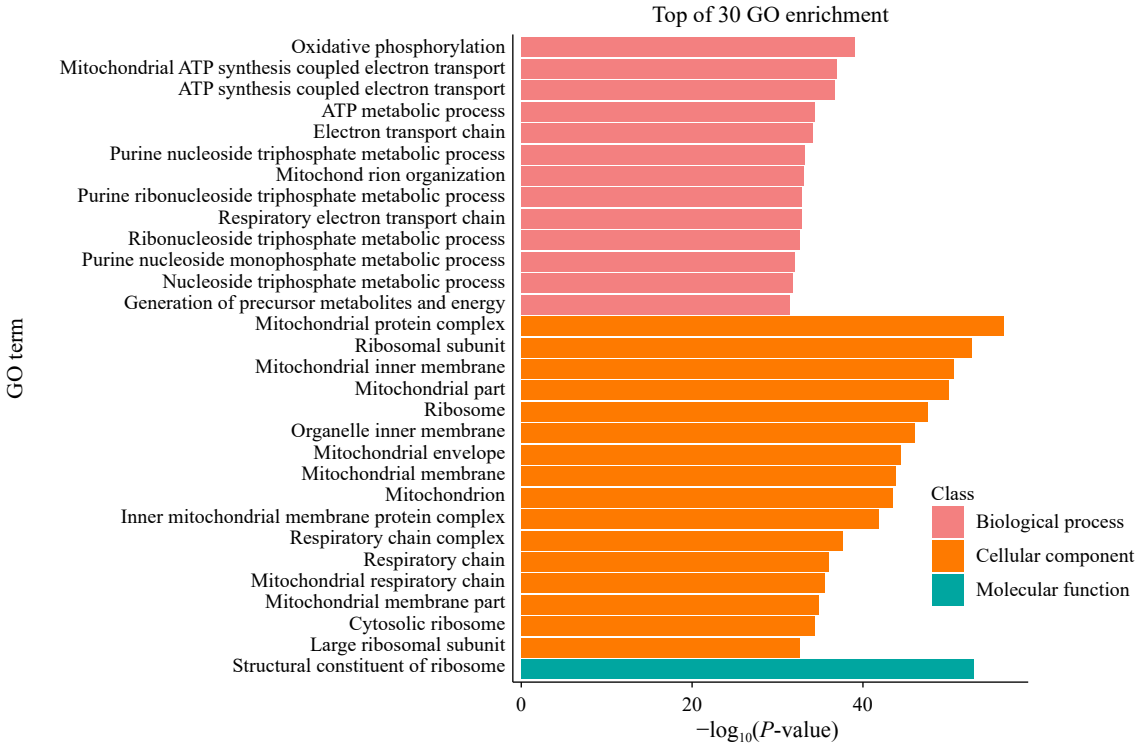

Fig.5 Gene ontology (GO) enrichment analysis of DEGs of the good and poor swimmers groups. The *x*-axis displays the $-\log_{10}$(*P*-value), while the *y*-axis represents the name of GO terms.

selected for RT-qPCR validation. Fig.7 illustrates the expression levels of each gene in both RT-qPCR and RNA-Seq. The results demonstrated a significant correlation between the expression patterns of these genes in RT-qPCR and RNA-seq analysis (correlation coefficient (R^2)=0.954, *P*-value<0.001), showing that the RT-qPCR expression results of the genes were consistent with the RNA-Seq data, which provides further confirmation of the reliability and accuracy of the RNA-Seq data.

4 Discussion

In the present study, the result of U_{crit} test revealed a significant discrepancy in swimming performance among different individuals of spotted sea bass juveniles. Intraspecies variation in swimming performance has been documented in various fish species, including large yellow croaker (*Larimichthys crocea*), shortnose sturgeon (*Aci-*

Table 5 List of 29 significantly enriched KEGG pathways

Term	Input number	Background number	*P*-value	Class		Rich factor
Ribosome	39	134	1.34E-34	Genetic information processing	Translation	0.291
Ribosome biogenesis in eukaryotes	5	77	0.0075	Genetic information processing	Translation	0.065
Mismatch repair	2	22	0.0487	Genetic information processing	Replication and repair	0.091
Fanconi anemia pathway	3	51	0.0458	Genetic information processing	Replication and repair	0.059
Sulfur relay system	2	8	0.0091	Genetic information processing	Folding, sorting and degradation	0.250
Cysteine and methionine metabolism	6	53	0.0002	Metabolism	Amino acid metabolism	0.113
Valine, leucine and isoleucine degradation	4	55	0.0114	Metabolism	Amino acid metabolism	0.073
Arginine and proline metabolism	4	61	0.0158	Metabolism	Amino acid metabolism	0.066
Tyrosine metabolism	3	34	0.0172	Metabolism	Amino acid metabolism	0.088
Tryptophan metabolism	3	50	0.0438	Metabolism	Amino acid metabolism	0.060
Glycolysis/Gluconeogenesis	7	77	0.0003	Metabolism	Carbohydrate metabolism	0.091
Citrate cycle (TCA cycle)	5	34	0.0003	Metabolism	Carbohydrate metabolism	0.147
Pyruvate metabolism	4	46	0.0064	Metabolism	Carbohydrate metabolism	0.087
Propanoate metabolism	3	34	0.0172	Metabolism	Carbohydrate metabolism	0.088
Glyoxylate and dicarboxylate metabolism	3	37	0.0212	Metabolism	Carbohydrate metabolism	0.081
Oxidative phosphorylation	38	140	8.82E-33	Metabolism	Energy metabolism	0.271
Sulfur metabolism	3	10	0.0008	Metabolism	Energy metabolism	0.300
Metabolic pathways	80	1507	4.91E-22	Metabolism	Global and overview maps	0.053
Carbon metabolism	11	132	9.93E-06	Metabolism	Global and overview maps	0.083
Biosynthesis of amino acids	5	88	0.0125	Metabolism	Global and overview maps	0.057
2-Oxocarboxylic acid metabolism	2	20	0.0415	Metabolism	Global and overview maps	0.100
Drug metabolism–cytochrome P450	3	34	0.0172	Metabolism	Xenobiotics biodegradation and metabolism	0.088
Metabolism of xenobiotics by cytochrome P450	3	37	0.0212	Metabolism	Xenobiotics biodegradation and metabolism	0.081
Glutathione metabolism	5	59	0.0026	Metabolism	Metabolism of other amino acids	0.085
Fatty acid degradation	3	46	0.0359	Metabolism	Lipid metabolism	0.065
Cardiac muscle contraction	15	117	1.27E-09	Organismal systems	Circulatory system	0.128
ECM-receptor interaction	12	89	3.48E-08	Environmental information processing	Signaling molecules and interaction	0.135
Focal adhesion	15	243	8.16E-06	Cellular processes	Cellular community–eukaryotes	0.062
AGE-RAGE signaling pathway in diabetic complications	6	127	0.0145	Human diseases	Endocrine and metabolic disease	0.047

penser brevirostrum), Atlantic cod (*Gadus morhua*), and European sea bass (*Dicentrarchus labrax*) (Nelson *et al*., 2002; Marras *et al*., 2010; Kieffer and May, 2020; Li *et al*., 2023). Previous research has demonstrated that the variation in swimming performance among different individuals of fish is both repeatable and statistically significant (Kolok, 1999). Swimming performance is closely associated with various fish behaviors, including predation, mate-finding, avoidance of adverse conditions, and Darwinian fitness (Drucker, 1996; Reidy *et al*., 2000; Plaut, 2001). Therefore, the observed individual discrepancies may reflect different adaptive strategies employed by fish to cope with complex and dynamic circumstances.

Furthermore, numerous studies have indicated that fish

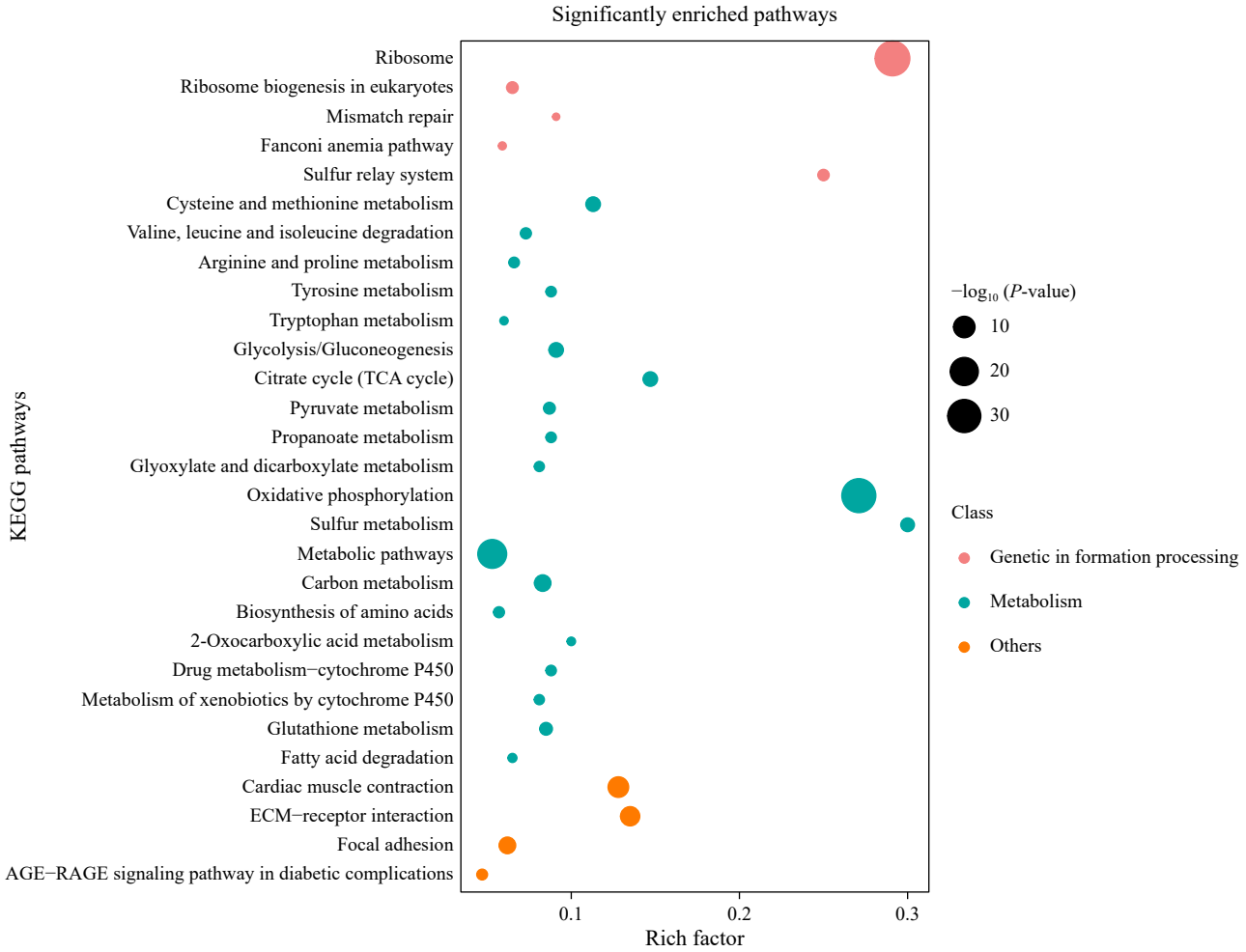

Fig.6 Kyoto Encyclopedia of Genes and Genomes (KEGG) enrichment analysis of DEGs in the good and poor swimmer groups. The *x*-axis shows the rich factor (DEGs enriched in a specific pathway compared to all genes in that pathway) and the *y*-axis represents the name of KEGG pathways. The sizes of each bubble correspond to the $-\log_{10}$(*P*-value) of the KEGG pathways.

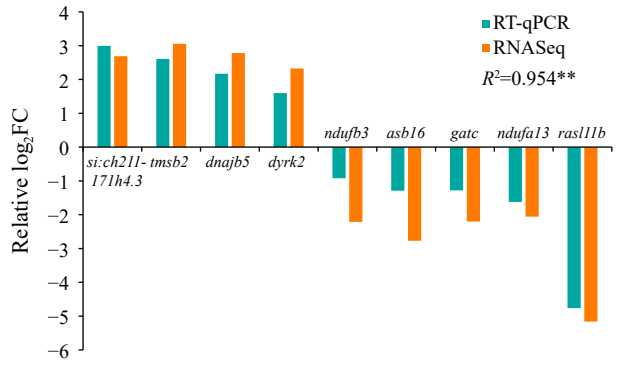

Fig.7 Validation of RNA-seq data *via* RT-qPCR. The relative $\log_2$FC of RT-qPCR results was compared with RNA-Seq. R^2 means the correlation coefficient, and ** indicates *P*-value<0.001. *18S rRNA* gene was used for normalization. The *x*-axis displays the name of genes, and the *y*-axis shows the relative $\log_2$FC levels. FC, fold change.

with superior swimming performance exhibit robustness, enhanced growth, increased disease resistance, and improved capacity to recover from acute stress, all of which contribute to the sustainable aquaculture (Merino *et al.*, 2007; McKenzie *et al.*, 2012; Castro *et al.*, 2013; Zeng *et al.*, 2022). Furthermore, moderate to high heritability of swimming performance has been reported in various fish species, including large yellow croaker (*Larimichthys crocea*), Nile tilapia (*Oreochromis niloticus*), and European sea bass (*Dicentrarchus labrax*) (Vandeputte *et al.*, 2016; Mengistu *et al.*, 2021; Zeng *et al.*, 2022). Therefore, it is reasonable to assume that swimming performance is a heritable trait in spotted sea bass, which could be utilized for selective breeding.

It is widely accepted that body weight and body length are positively correlated with swimming performance, which are consistant with our findings (Cai *et al.*, 2020; Cano-Barbacil *et al.*, 2020). Additionally, the condition factor (BW/BL) exhibited a significant positive correlation with absolute U_{crit} in this study, suggesting that muscle development may significantly impact swimming performance. The caudal region, specifically the caudal fin, plays a vital role in fish locomotion (Webb, 1984). In this study, a positive correlation was observed between absolute U_{crit} and CRL/TL, indicating that a longer caudal region benefits individual swimming performance. This is consistent with the findings in brown trout (*Salmo trutta* L.), where individuals with longer caudal regions exhibit-

ed superior swimming performance (Ojanguren and Brana, 2003). In contrast, CPL/TL showed no correlation with absolute U_{crit}, suggesting that the anterior portion of the caudal region, rather than the caudal peduncle, plays a crucial role in swimming performance. Additionally, CFL and CFL/TL exhibited distinct correlations with absolute U_{crit} (correlation coefficient, CFL: 0.23, CFL/TL: −0.13), indicating that while the caudal fin is essential for swimming, a relatively longer caudal fin may hinder swimming performance among individuals of the same body size. Similarly, a study involving zebrafish found that excessively long caudal fins hindered forward movement as they impeded the generation of driving force; however, it's interesting that excessively short caudal fins are also detrimental to swimming performance (Wakamatsu *et al*., 2019). Thus, a caudal fin of moderate length is necessary for optimizing swimming performance.

In our study, although PFL showed no significant correlation with absolute U_{crit}, a negative correlation was observed between PFL/TL and absolute U_{crit} (correlation coefficient, PFL/TL: −0.15), suggesting that individuals with better swimming performance tend to have shorter pectoral fins relative to their total length. Similarly, this trend was found in brook trout (*Salvelinus fontinalis*, Mitchill) as well (Rouleau *et al*., 2010). We hypothesize that while the pectoral fin plays a crucial role in altering swimming direction, it may impede swimming speed during forward movement due to the drag force generated by its surface. Furthermore, though head length and torso length show a significant positive correlation with swimming performance, HL/TL and ToL/TL had no significant correlation with absolute U_{crit} statistically, indicating that the proportion of head and torso have a limited influence on the swimming performance of spotted sea bass.

Swimming is an energy-intensive process, powered by the aerobic metabolism of muscles (Chai *et al*., 2023). In this study, we found that the majority of DEGs were enriched in GO terms related to mitochondrial energy metabolism and KEGG pathways related to oxidative phosphorylation, suggesting that mitochondrial energy metabolism may substantially contribute to the observed differences in swimming performance among fish. Similarly, the oxidative phosphorylation pathway was identified as the most enriched KEGG pathway in large yellow croaker (*Larimichthys crocea*) with varying swimming performances (Li *et al*., 2023). Additionally, research has shown that fish species exhibiting high swimming performance demonstrate greater oxidative phosphorylation efficiency compared to species with lower swimming performance (Zhang and Broughton, 2015).

The KEGG pathways analysis revealed the correlation of carbohydrate metabolism (Glycolysis/Gluconeogenesis, Citrate cycle (TCA cycle), Pyruvate metabolism, Propanoate metabolism, Glyoxylate and dicarboxylate metabolism) with the variation of swimming performance among fishes. Previous research has shown that fish with superior swimming performance tend to exhibit higher blood glucose levels (Chai *et al*., 2023). For instance, juvenile tinfoil barb (*Barbonymus schwanenfeldii* (Bleeker, 1854)) under high-speed sustained training stimulated glycolysis, increased activities of hexokinase, pyruvate kinase and reduced glycogen in white muscle and liver; in juvenile rainbow trout (*Oncorhynchus mykiss*), the proportion of carbohydrates in all fuel burned during sustained swimming increased with the swimming speed approach to U_{crit} (Lauff and Wood, 1996; Zhu *et al*., 2016). Integrating our findings, we hypothesize that juveniles of spotted sea bass with superior swimming performance may catabolize glycogen to improve their blood glucose levels, therefore, they could produce more energy to support their intenser locomotion. Furthermore, amino acid metabolism (including cysteine and methionine metabolism, valine, leucine and isoleucine degradation, arginine and proline metabolism, tyrosine metabolism, and tryptophan metabolism) was also correlated with individual differences of swimming performance. Early studies have demonstrated the significant role of protein as a metabolic fuel during aerobic swimming in fish, although this has been attributed to the scarcity of carbohydrates (Magnoni *et al*., 2013). For example, in the contracting muscle of swimming trout (*Salmo gairdneri*), leucine appears to be preferred for oxidation (van den Thillart, 1986). Under high speed flow velocity exercise, KEGG functional pathway of Chinese perch (*Siniperca chuatsi*) was mainly mapped to amino acid metabolism (Zhu *et al*., 2023). Therefore, by satisfying the requirements of fish for carbohydrates, it may be possible to reduce their reliance on protein and amino acid consumption. In addition, our study revealed a correlation between swimming performance and lipid metabolism, specifically fatty acid degradation, indicating that lipids serve as a primary metabolic fuel for sustained swimming (Lauff and Wood, 1996; Magnoni *et al*., 2013).

A significant enrichment in ribosome-related terms and pathways was observed in this study, including ribosomal subunit, cytosolic ribosome, and KEGG pathways related to the ribosome and ribosome biogenesis in eukaryotes. Notably, these enrichment associated with ribosomes exhibited a remarkably low *P*-value herein. Likewise, due to swimming exercise, increase of ribosomal and transcriptional capacities was observed in gilthead sea bream (*Sparus aurata*) (Martin-Perez *et al*., 2012). Based on our results and previous findings, it is plausible that enhanced swimming performance in fish may be linked to the upregulation of ribosomal translation efficiency, which facilitates protein synthesis. This adaptive response likely serves to meet the increased demands for growth and energy metabolism associated with vigorous swimming activities.

Cardiac muscle contraction plays an essential role in pumping blood throughout the closed circulatory system to ensure sufficient oxygenation and nutrition in vertebrates (Vornanen *et al*., 2002). Our KEGG pathway analysis result showed a close association between the cardiac muscle contraction pathway and swimming performance. Similarly, rainbow trout (*Oncorhynchus mykiss*) exhibiting superior swimming performance demonstrated higher maximum *in vivo* cardiac output and maximum car-

diac power output (Claireaux *et al*., 2005). Therefore, individuals with better swimming performance might have a tendency to exhibit more robust cardiac muscle.

5 Conclusions

Specific morphological phenotypes of individual spotted sea bass can impact their swimming performance. A significant discrepancy in swimming performance was observed among spotted sea bass individuals. Among juveniles of equivalent total length, good swimmers exhibited longer caudal regions, higher condition factors, and shorter caudal and pectoral fins. At the genetic level, the transcriptomes of the white muscle in spotted sea bass exhibiting varying swimming performances were analyzed. A total of 694 DEGs were identified, which were predominantly enriched in biological processes related to energy metabolism, structural constituents of ribosomes, and cardiac muscle contraction. This research deepens our understanding of the mechanisms underlying swimming performance in spotted sea bass regarding morphology and genetics. It is helpful for selecting suitable spotted sea bass breeds for deep-sea aquaculture.

Acknowledgements

This research was funded by the National Key R&D Program of China (No. 2022YFD2400103). We would like to thank Mr. Yonghang Zhang, Mr. Chao Zhai, Dr. Kaiqiang Zhang, Mr. Tianyu Jiang, Ms. Chaonan Sun and other laboratory members for providing methodological guidance.

Author Contributions

Haoyang Li: completion of the experiment, formal analysis, data analysis, visualization, and manuscript drafting. Hao Li: resources, completion of the experiment, data analysis, visualization, and manuscript revising. Chengtian Li: completion of the experiment, validation, and manuscript drafting. Xi Jin: completion of the experiment, and manuscript drafting. Weiwei Li: completion of the experiment. Haishen Wen: conceptualization. Yun Li: conceptualization. Qianyan Lai: completion of the experiment. Chunxiang Niu: completion of the experiment. Xin Qi: supervision, methodology, funding acquisition, and manuscript revising.

Data Availability

The data and references presented in this study are available from the corresponding author upon reasonable request.

Declarations

Ethics Approval and Consent to Participate

All experimental spotted sea bass were housed and treated in accordance with the guidelines of the Animal Research and Ethics Committees of Ocean University of China (Permit number: 20141201). And there were no endangered or protected species in the present study.

Consent for Publication

Informed consent for publication was obtained from all participants.

Conflict of Interests

The authors declare that they have no conflict of interests.

References

Anders, S., and Huber, W., 2010. Differential expression analysis for sequence count data. *Genome Biology*, **11**: R106.

Barclay, C. J., 2019. *Muscle and Exercise Physiology*. Academic Press, Pittsburgh, 111-127.

Brett, J. R., 1964. The respiratory metabolism and swimming performance of young sockeye salmon. *Journal of the Fisheries Research Board of Canada*, **21**: 1183–1226.

Bu, D., Luo, H., Huo, P., Wang, Z., Zhang, S., He, Z., *et al*., 2021. KOBAS-i: Intelligent prioritization and exploratory visualization of biological functions for gene enrichment analysis. *Nucleic Acids Research*, **49** (W1): W317–W325.

Cai, L., Chen, J., Johnson, D., Tu, Z., and Huang, Y., 2020. Effect of body length on swimming capability and vertical slot fishway design. *Global Ecology and Conservation*, **22**: e00990.

Cano-Barbacil, C., Radinger, J., Argudo, M., Rubio-Gracia, F., Vila-Gispert, A., and Garcia-Berthou, E., 2020. Key factors explaining critical swimming speed in freshwater fish: A review and statistical analysis for Iberian species. *Scientific Reports*, **10**: 18947.

Castro, V., Grisdale-Helland, B., Jorgensen, S. M., Helgerud, J., Claireaux, G., Farrell, A. P., *et al*., 2013. Disease resistance is related to inherent swimming performance in Atlantic salmon. *BMC Physiology*, **13**: 1.

Chai, R., Yin, H., Huo, R., Wang, H., Huang, L., and Wang, P., 2023. Effects of constant water flow on endurance swimming and fatigue metabolism of large yellow croaker. *Journal of Marine Science and Engineering*, **11**: 270.

Chen, C., Liu, H., Huang, Y., Yang, J., Liang, X., Zhang, C., *et al*., 2019. Numerical simulation of mechanical characteristics of a metal net for deep-sea aquaculture. *Journal of Ocean University of China*, **18**: 1273–1281.

Chen, C., Wu, Y., Li, J., Wang, X., Zeng, Z., Xu, J., *et al*., 2023. TBtools-II: A 'one for all, all for one' bioinformatics platform for biological big-data mining. *Molecular Plant*, **16**: 1733–1742.

Chen, C., Yan, H., Zhang, T., and Su, Y., 2022. Swimming ability and behavior of *Anguilla japonica*. *Journal of Hydroecology*, **43**: 4 (in Chinese with English abstract).

Chen, S., Zhou, Y., Chen, Y., and Gu, J., 2018. fastp: An ultra-fast all-in-one FASTQ preprocessor. *Bioinformatics*, **34**: i884–i890.

Claireaux, G., McKenzie, D. J., Genge, A. G., Chatelier, A., Aubin, J., and Farrell, A. P., 2005. Linking swimming performance, cardiac pumping ability and cardiac anatomy in rainbow trout. *Journal of Experimental Biology*, **208**: 1775–1784.

Domenici, P., Herbert, N., Lefrançois, C., Steffensen, J., and

McKenzie, D., 2013. *Swimming Physiology of Fish*. Springer, Berlin, Heidelberg, 129–159.

Dong, G., Zheng, Y., Li, Y., Teng, B., Guan, C., and Lin, D., 2008. Experiments on wave transmission coefficients of floating breakwaters. *Ocean Engineering*, **35**: 931–938.

Drucker, E. G., 1996. The use of gait transition speed in comparative studies of fish locomotion. *American Zoologist*, **36**: 555–566.

Gentry, R. R., Lester, S. E., Kappel, C. V., White, C., Bell, T. W., Stevens, J., *et al*., 2017. Offshore aquaculture: Spatial planning principles for sustainable development. *Ecology and Evolution*, **7**: 733–743.

Gui, F., Wang, P., and Wu, C., 2014. Evaluation approaches of fish swimming performance. *Agricultural Sciences*, **5**: 106–113.

Faulkner, J. A., Davis, C. S., Mendias, C. L., and Brooks, S. V., 2008. The aging of elite male athletes: Age-related changes in performance and skeletal muscle structure and function . *Clinical Journal of Sport Medicine*, **18**: 501–507.

Furrer, R., Hawley, J. A., and Handschin, C., 2023. The molecular athlete: Exercise physiology from mechanisms to medals. *Physiological Reviews*, **103** (3): 1693–1787.

Hammer, C., 1995. Fatigue and exercise tests with fish. *Comparative Biochemistry and Physiology Part A: Physiology*, **112**: 1–20.

Hvas, M., Folkedal, O., and Oppedal, F., 2021. Fish welfare in offshore salmon aquaculture. *Reviews in Aquaculture*, **13**: 836–852.

Jhonnerie, R., Yani, A. H., and Fatmawati, R., 2023. Behavior and swimming performance of local fish in the ecosystem waters of rivers, oxbow and peat swamps. *Journal of Animal Behaviour and Biometeorology*, **11**: e2023002–e2023002.

Kieffer, J. D., and May, L. E., 2020. Repeat U_{crit} and endurance swimming in juvenile shortnose sturgeon (*Acipenser brevirostrum*). *Journal of Fish Biology*, **96**: 1379–1387.

Kim, D., Langmead, B., and Salzberg, S. L., 2015. HISAT: A fast spliced aligner with low memory requirements. *Nature Methods*, **12**: 357–360.

Kolok, A., 1999. Interindividual variation in the prolonged locomotor performance of ectothermic vertebrates: A comparison of fish and herpetofaunal methodologies and a brief review of the recent fish literature. *Canadian Journal of Fisheries and Aquatic Sciences*, **56**: 700–710.

Lauff, R., and Wood, C., 1996. Respiratory gas exchange, nitrogenous waste excretion, and fuel usage during aerobic swimming in juvenile rainbow trout. *Journal of Comparative Physiology B*, **166**: 501–509.

Li, H., Handsaker, B., Wysoker, A., Fennell, T., Ruan, J., Homer, N., *et al*., 2009. The sequence alignment/map format and SAMtools. *Bioinformatics*, **25**: 2078–2079.

Li, Q., Wen, H., Li, Y., Zhang, Z., Zhou, Y., and Qi, X., 2019. Evidence for the direct effect of the NPFF peptide on the expression of feeding-related factors in spotted sea bass (*Lateolabrax maculatus*). *Front Endocrinol (Lausanne)*, **10**: 545.

Li, S., Liu, X., Lin, T., Feng, G., Wang, X., and Zhang, D., 2023. Muscle fiber plasticity, stress physiology, and muscle transcriptome determine the inter-individual difference of swimming performance in the large yellow croaker (*Larimichthys crocea*). *Aquaculture*, **567**: 739247.

Liao, Y., Smyth, G. K., and Shi, W., 2014. featureCounts: An efficient general purpose program for assigning sequence reads to genomic features. *Bioinformatics*, **30**: 923–930.

Liu, J. X., Gao, T. X., Yokogawa, K., and Zhang, Y. P., 2006. Differential population structuring and demographic history of two closely related fish species, Japanese sea bass (*Lateolabrax japonicus*) and spotted sea bass (*Lateolabrax maculatus*) in Northwestern Pacific. *Molecular Phylogenetics and Evolution*, **39**: 799–811.

Liu, Y., Wang, H., Wen, H., Shi, Y., Zhang, M., Qi, X., *et al*., 2020. First high-density linkage map and QTL fine mapping for growth-related traits of spotted sea bass (*Lateolabrax maculatus*). *Marine Biotechnology (NY)*, **22**: 526–538.

Livak, K. J., and Schmittgen, T. D., 2001. Analysis of relative gene expression data using real-time quantitative PCR and the $2^{-\Delta\Delta CT}$ method. *Methods*, **25**: 402–408

Long, L., Liu, H., Cui, M., Zhang, C., and Liu, C., 2024. Offshore aquaculture in China. *Reviews in Aquaculture*, **16**: 254–270.

Love, M. I., Huber, W., and Anders, S., 2014. Moderated estimation of fold change and dispersion for RNA-seq data with DESeq2. *Genome Biology*, **15**: 550.

Magnoni, L., Felip, O., Blasco, J., and Planas, J., 2013. *Swimming Physiology of Fish*. Springer, Berlin, Heidelberg, 203–235.

Marras, S., Claireaux, G., McKenzie, D. J., and Nelson, J. A., 2010. Individual variation and repeatability in aerobic and anaerobic swimming performance of European sea bass *Dicentrarchus labrax*. *Journal of Experimental Biology*, **213**: 26–32.

Martin-Perez, M., Fernandez-Borras, J., Ibarz, A., Millan-Cubillo, A., Felip, O., de Oliveira, E., *et al*., 2012. New insights into fish swimming: A proteomic and isotopic approach in gilthead sea bream. *Journal of Proteome Research*, **11**: 3533–3547.

Martinez, M., Guderley, H., Dutil, J. D., Winger, P. D., He, P., and Walsh, S. J., 2003. Condition, prolonged swimming performance and muscle metabolic capacities of cod *Gadus morhua*. *Journal of Experimental Biology*, **206**: 503–511.

McClelland, G. B., Craig, P. M., Dhekney, K., and Dipardo, S., 2006. Temperature- and exercise-induced gene expression and metabolic enzyme changes in skeletal muscle of adult zebrafish (*Danio rerio*). *The Journal of Physiology*, **577**: 739–751.

McKenzie, D. J., Höglund, E., Dupont-Prinet, A., Larsen, B. K., Skov, P. V., Pedersen, P. B., *et al*., 2012. Effects of stocking density and sustained aerobic exercise on growth, energetics and welfare of rainbow trout. *Aquaculture*, **338**: 216–222.

Mengistu, S. B., Palstra, A. P., Mulder, H. A., Benzie, J. A. H., Trinh, T. Q., Roozeboom, C., *et al*., 2021. Heritable variation in swimming performance in Nile tilapia (*Oreochromis niloticus*) and negative genetic correlations with growth and harvest weight. *Scientific Reports*, **11**: 11018.

Merino, G. E., Piedrahita, R. H., and Conklin, D. E., 2007. Effect of water velocity on the growth of California halibut (*Paralichthys californicus*) juveniles. *Aquaculture*, **271**: 206–215.

Ministry of Agriculture and Rural Affairs, PRC, 2023. *China Fishery Statistical Yearbook*. China Agriculture Press, Beijing, 2–22.

Nelson, J. A., Gotwalt, P. S., Reidy, S. P., and Webber, D. M., 2002. Beyond $U_{(crit)}$: Matching swimming performance tests to the physiological ecology of the animal, including a new fish 'drag strip'. *Comparative Biochemistry and Physiology Part A: Molecular & Integrative Physiology*, **133**: 289–302.

Ohlberger, J., Staaks, G., and Holker, F., 2006. Swimming efficiency and the influence of morphology on swimming costs in fishes. *Journal of Comparative Physiology B*, **176**: 17–25.

Ojanguren, A. F., and Brana, F., 2003. Effects of size and morphology on swimming performance in juvenile brown trout

(*Salmo trutta* L.). *Ecology of Freshwater Fish*, **12**: 241–246.

Plaut, I., 2001. Critical swimming speed: Its ecological relevance. *Comparative Biochemistry and Physiology Part A: Molecular & Integrative Physiology*, **131**: 41–50.

Raffini, F., Schneider, R. F., Franchini, P., Kautt, A. F., and Meyer, A., 2020. Diving into divergence: Differentiation in swimming performances, physiology and gene expression between locally-adapted sympatric cichlid fishes. *Molecular Ecology*, **29**: 1219–1234.

Reidy, S. P., Kerr, S. R., and Nelson, J. A., 2000. Aerobic and anaerobic swimming performance of individual Atlantic cod. *Journal of Experimental Biology*, **203**: 347–357.

Rouleau, S., Glémet, H., and Magnan, P., 2010. Effects of morphology on swimming performance in wild and laboratory crosses of brook trout ecotypes. *Functional Ecology*, **24**: 310–321.

Rubio-Gracia, F., Garcia-Berthou, E., Guasch, H., Zamora, L., and Vila-Gispert, A., 2020. Size-related effects and the influence of metabolic traits and morphology on swimming performance in fish. *Current Zoology*, **66**: 493–503.

Sun, Z., Li, S., Liu, Y., Li, W., Liu, K., Cao, X., *et al*., 2024. Telomere-to-telomere gapless genome assembly of the Chinese sea bass (*Lateolabrax maculatus*). *Scientific Data*, **11**: 175.

Suchomel, T. J., Nimphius, S., and Stone, M. H., 2016. The importance of muscular strength in athletic performance. *Sports Medicine*, **46**: 1419–1449.

Tetsuo Kawai, D., and Morihiko, S., 1996. Fish flavor. *Critical Reviews in Food Science and Nutrition*, **36**: 257–298.

Timmerhaus, G., Lazado, C. C., Cabillon, N. A. R., Reiten, B. K. M., and Johansen, L. H., 2021. The optimum velocity for Atlantic salmon post-smolts in RAS is a compromise between muscle growth and fish welfare. *Aquaculture*, **532**: 736076.

van den Thillart, G., 1986. Energy metabolism of swimming trout (*Salmo gairdneri*) oxidation rates of palmitate, glucose, lactate, alanine, leucine and glutamate. *Journal of Comparative Physiology B*, **156**: 511–520.

Vandeputte, M., Porte, J., Aupérin, B., Dupont-Nivet, M., Vergnet, A., Valotaire, C., *et al*., 2016. Quantitative genetic variation for post-stress cortisol and swimming performance in growth-selected and control populations of European sea bass (*Dicentrarchus labrax*). *Aquaculture*, **455**: 1–7.

Vornanen, M., Shiels, H. A., and Farrell, A. P., 2002. Plasticity of excitation-contraction coupling in fish cardiac myocytes. *Comparative Biochemistry and Physiology Part A: Molecular & Integrative Physiology*, **132**: 827–846.

Wakamatsu, Y., Ogino, K., and Hirata, H., 2019. Swimming capability of zebrafish is governed by water temperature, caudal fin length and genetic background. *Scientific Reports*, **9**: 16307.

Wang, H., Wen, H., Li, Y., Zhang, K., and Liu, Y., 2018. Evaluation of potential reference genes for quantitative RT-PCR analysis in spotted sea bass (*Lateolabrax maculatus*) under normal and salinity stress conditions. *PeerJ*, **6**: e5631.

Webb, P. W., 1984. Body form, locomotion and foraging in aquatic vertebrates. *American Zoologist*, **24**: 107–120.

Xie, S., Zhou, Q., Zhang, X., Zhu, T., Guo, C., Yang, Z., *et al*., 2022. Effect of dietary replacement of fish meal with low-gossypol cottonseed protein concentrate on growth performance and expressions of genes related to protein metabolism for swimming crab (*Portunus trituberculatus*). *Aquaculture*, **549**: 737820.

Yan, W., Huang, L., Li, Y., Wang, G., Wu, Q., and You, X., 2022. Hydrodynamic characteristics of rainbow trout (*Oncorhynchus mykiss*). *Fishery Modernization*, **49** (3): 36–45.

Yuan, X., Wang, C., Miao, Q., and Zou, C., 2023. Effects of variable porosity net on flow field inside deep-sea aquaculture cage. *IOP Conference Series: Materials Science and Engineering*, **1288**: 012034.

Zeng, J., Long, F., Wang, J., Zhao, J., Ke, Q., Gong, J., *et al*., 2022. GWAS reveals heritable individual variations in the inherent swimming performance of juvenile large yellow croaker. *Aquaculture*, **559**: 738419.

Zhang, F., and Broughton, R. E., 2015. Heterogeneous natural selection on oxidative phosphorylation genes among fishes with extreme high and low aerobic performance. *BMC Ecology and Evolution*, **15**: 1–15.

Zhang, X., Wen, H., Wang, H., Ren, Y., Zhao, J., and Li, Y., 2017. RNA-Seq analysis of salinity stress-responsive transcriptome in the liver of spotted sea bass (*Lateolabrax maculatus*). *PLoS One*, **12**: e0173238.

Zhang, Z., and Liu, Y., 2018. The status quo, issues and foreign experiences of deep sea aquaculture equipment of China. *Proceedings of 2018 2nd International Conference on Social Sciences, Arts and Humanities (SSAH 2018)*. Tianjin, 397–401.

Zhu, T., Yang, R., Xiao, R., Ni, W., Liu, L., Zhao, J., *et al*., 2023. Effect of swimming training on the flesh quality in Chinese perch (*Siniperca chuatsi*) and its relationship with muscle metabolism. *Aquaculture*, **577**: 739926.

Zhu, Z., Song, B., Lin, X., and Xu, Z., 2016. Effect of sustained training on glycolysis and fatty acids oxidation in swimming muscles and liver in juvenile tinfoil barb *Barbonymus schwanenfeldii* (Bleeker, 1854). *Fish Physiology and Biochemistry*, **42**: 1807–1817.

(Edited by Qiu Yantao)